Mexican
Journal
of
Phytopathology
e-ISSN: 2007-8080

Crossref
Open access

Scientific Article

Characterization of *Sclerotium rolfsii* and species of *Trichoderma* in commercial crops of potato in Sonora and Sinaloa, Mexico

María Belén Irazoqui-Acosta[1], **Rubén Felix-Gastelum**[1*], **Karla Yeriana Leyva-Madrigal**[1], **Rosa Maria Longoria-Espinoza**[1], **Gabriel Herrera-Rodríguez**[2], **Sara Elodia Armenta-López**[2]. [1]Universidad Autónoma de Occidente, Unidad Los Mochis, Departamento de Ciencias Naturales y Exactas, Boulevard Macario Gaxiola y Carretera Internacional, S/N, Los Mochis, Sinaloa, CP. 81223. [2]Junta Local de Sanidad Vegetal del Valle del Fuerte. Lázaro Cárdenas, 315 Pte. Col. Centro, Los Mochis Sinaloa, CP. 81200. México.

***Corresponding Author:**
Rubén Félix-Gastelum
ruben.felix@uadeo.mx

Section:
Periodical Issue

Received:
August 09, 2024
Accepted:
August 22, 2025
Published:
August 28, 2025

Citation:
Irazoqui-Acosta MB, Félix-Gastelum R, Leyva-Madrigal KY, Longoria-Espinoza RM, Herrera-Rodríguez G, *et al*. 2025. Characterization of *Sclerotium rolfsii* and species of *Trichoderma* in commercial crops of potato in Sonora and Sinaloa, Mexico. Mexican Journal of Phytopathology 43(3): 85. https://doi.org/10.18781/R.MEX.FIT.2408-1

ABSTRACT

Background/Objective. *Sclerotium rolfsii* causes losses in potato production up to 20% in the states of Sonora and Sinaloa. No studies exist supported by the scientific method on the identification of the fungus in the crop, neither of the species of *Trichoderma* present in the soil with potential to control the disease under field conditions. The objectives of the present study were to: a) obtain isolates of *S. rolfsii* from soil subject to the potato crop in the states of Sonora and Sinaloa, and determine the population density of sclerotia of the fungus; isolate and quantify the population density of *Trichoderma* spp., in the same soil to use them in subsequent studies for controlling the disease and determine the pathogenicity of *S. rolfsii* in potato tubers under laboratory conditions.

Materials and Methods. The isolates were collected from 239 commercial potato fields in the states of Sonora and Sinaloa. The population density was determined by counting the sclerotia of *S. rolfsii* and the colony forming units (CFU g^{-1}) of *Trichoderma* in soil. The identification of the fungi was performed by morphological studies and molecular techniques including the internal transcribed spacer (ITS) for *S. rolfsii* and the subunit of RNA polymerase II (RPB2) for *Trichoderma spp*. The pathogenicity tests of the isolates of *S. rolfsii* were determined in potato tubers var. Fianna in the laboratory.

Results. Twenty isolates of *S. rolfsii* were identified whose population density varied from 2 to 24 sclerotia kg^{-1} of soil. On the other hand, 26 isolates of *Trichoderma* spp. were identified; 16 of them corresponded to *T. asperellum*, five to *T. asperelloides*, four to T. *afroharzianum* and one to *T. azevedoi* with a population density from 2 to 8 CFU g^{-1} of soil. The isolates of *S. rolfsii* resulted pathogenic to potato tubers var. Fianna, with different levels of aggressiveness.

Conclusion. The results obtained in the present study indicate the presence of *S. rolfsii* in 8.4% of the 239 potato growing fields included in the study sampled in the growing cycles 2019-2022 con population densities from 2 to 24 sclerotia g^{-1} of soil. The pathogen confirmation by conventional and molecular techniques, as well as its capability to induce soft rot of potato tubers var. Fianna, provides evidence of its potential impact on potato production. Variable aggressiveness was detected among isolates, highlighting the Scr4 isolate as the most aggressive with penetration up to 16.9 mm and soft rotting of 10.5%. In parallel, 26 isolates of *Trichoderma* spp. were identified in 10.9% of the fields, with population densities from 2 to 8 CFU g^{-1} of soil. These findings highlight the importance of incorporating sustainable strategies for disease management, considering both the variability of the pathogen and the possible application of native antagonists; also, it is stressed the necessity to investigate the population dynamics of the pathogen and agricultural practices to minimize its survival.

Keywords. Fungi, Identification, Population density, Pathogenicity, Virulence

INTRODUCTION

The potato (*Solanum tuberosum*) is considered one of the most important crops, due to its worldwide production, after wheat (*Triticum* spp.) and rice (*Oryza sativa*) (FAO, 2024). In Mexico, potato production is estimated in 1,986,198 t (SIAP, 2023), with the states of Sonora and Sinaloa being the main producers, and in which the Fianna, Orquesta, Atlantic, FL-1867, FL-2027, FL-2395 and FL-2312 varieties stand out, accounting for 52.4% of the country's production (SIAP, 2023). Yield is determined by diverse factors in crop management, the most outstanding of which include diseases of biotic origin, which affect plant development and the quality of the tubers (Herrera and Scott, 1993). The fungi, bacteria, nematodes and viruses that affect the tuber produce foliar spots, galls, mosaics, rots and others (Fiers *et al*., 2012).

Soft rot is a disease caused by the fungus *Sclerotium rolfsii*. The symptoms consist of maroon lesions in the stem and tubers, and in advanced stages of the disease, soft rot is found, with slightly sunken lesions. Signs are characterized by the development of white mycelia and the presence of round maroon sclerotia, between 2 and 4 mm in diameter on the infected tissue (Garibaldi *et al*., 2007; Roca *et al*., 2016). Losses caused by the disease have reached up to 60% in other parts of the world (Haque and Khan, 1977). In Sinaloa, damages have been estimated in 20% in commercial potato plantations.

S. rolfsii is a necrotrophic fungus that lives in the soil, with a high capacity of saprophytic growth. It is considered a pathogen of high economic importance in agriculture, due to its wide range of hosts, wide geographic distribution and ability for survival due to its formation of sclerotia and mycelia, allowing it to survive in dead organic matter or alternative hosts (Aycock, 1966; Punja, 1985).

In recent years, in the states of Sinaloa and Sonora, symptoms of soft rot have been found in potato crops. It is worth mentioning that studies have been carried out for the control of this disease, in which the adequate doses of fungicide have been determined for its control (Browne *et al*., 2002). However, the high cost, environmental regulations and the toxicity of the fumigants limit the use of this type of molecules in the management of this disease (García-González *et al*., 2022). The application of *Trichoderma* species as biocontrol agents has also been used, and they have proven to be effective (Guzmán *et al*., 2014; Zúñiga and Ceja, 2017). Martínez-Martínez *et al*. (2020) carried out a study in Mexico, in which different strains of different species of *Trichoderma* were used against the mycelial growth of *S. rolfsii*, resulting in a viable alternative, both *in vitro* and *in planta* for the control of this phytopathogen in chickpea. Nevertheless, no research has been carried out in Mexico on this disease on potato crops.

Due to this, the aims of this study were: a) to obtain *S. rolfsii* isolates from soils under potato cultivation in the states of Sonora and Sinaloa, and to determine the population density of the fungal sclerotia; b) to isolate, quantify the population density and morphologically and molecularly identify *Trichoderma* spp. isolates from the same soils in order to use them in subsequent studies for disease control; and d) to determine the pathogenicity of *S. rolfsii* in potato tubers under laboratory conditions.

MATERIALS AND METHODS

Gathering samples. During the development of the study, soil samples were obtained from 239 plots in which potato is produced in Sonora and Sinaloa, in the 2019-2020, 2020-2021 and 2021-2022 autumn-winter growing seasons. Ten-hectare plots were selected from which 500 g subsamples were collected using the method known as "five-point sampling". The samples were homogenized, taking 1 kg as a final sample.

Population density, isolation and morphological characterization of *S. rolfsii* isolates. In order to determine the *S. rolfsii* populations, sclerotia were extracted from the soil samples using the Fenwick can technique (Van-Bezooijen, 2006). A soil sample weighing 500 g was placed in a number 20 (850 µm) sieve, on the can. In the water output, a number 60 sieve was placed (250 µm). Subsequently, the retained particles were dried in the shade over absorbent paper for 24 h. The particles were observed under a stereoscopic microscope (Carl Zeiss®; SteREO Discovery.V20, Germany); the sclerotia obtained in the sample were then collected and quantified. Next, they were disinfested in a 1% sodium hypochlorite solution for one minute and planted in a Potato Dextrose Agar (PDA) culture medium (BD Bioxon®) supplemented with chloramphenicol (15 µg mL^{-1}) (Armenta-López *et al.,* 2021). The dishes were incubated at 27 °C for 48 h (Yamato Scientific Co., LTD®; Economy Incubator IN804, Tokyo, Japan). From the growth point of the colony, a disk with 5 mm in diameter was taken and transferred into Petri dishes containing PDA and then incubated at 27 °C.

For the morphological identification of *Sclerotium* spp., a PDA disk, 5 mm in diameter and with active growth from each isolate, was placed on the edge of three 90 mm Petri dishes with the same medium. The dishes were incubated at 27 °C until the fungus filled the dish. To determine the mycelial growth rate, the following formula was used: TC = (Final growth – Initial growth) / time of incubation (Guigón–López *et al*., 2010). The colonial morphology was described: color of colony in the dish (front and back); mycelium shape and type. The characteristics of the hyphae and the formation of the fibulae and the color of the sclerotia were also recorded (Paparu *et al.,* 2020). Additionally, the average number of sclerotia produced was evaluated and the size of 30 of them was determined per Petri dish in each one of the isolates (Prasad *et al.,* 2012).

Population density, isolation and morphological characterization of *Trichoderma* spp. isolates. In order to obtain *Trichoderma* spp. isolates, 0.5 g of soil from each sample were weighed (Ohaus Corporation®; YS600, China), sprinkled over the surface of a Petri dish with PDA and incubated for 10 days at 27 °C. Once the colonies with a typical morphology for the genus developed (Gary and Prakash, 2015), they were quantified in each Petri dish, transferred into dishes with the same medium and incubated at 27 °C. The *Trichoderma* colonies were purified using the monosporic culture technique by Estrada *et al.* (1997). From every *Trichoderma* isolate, two 5-mm mycelium disks were transferred to PDA, Spezieller Nährstoffarmer Agar (SNA) (modified by Nirenberg, 1976) and Corn Meal Agar (CMA) (BD BBL®), on the edge of Petri dishes, 90 mm in diameter (three replications for every medium). The dishes were incubated for seven days in a bioclimatic chamber (Thermo Scientific®; Precision 3759, USA), using cold white fluorescent light at 25 °C (Pacheco *et al.,* 2016). Mycelial growth was measured every 24 h until it covered the Petri plates with PDA and SNA. Measurements were taken from the edge of the inoculum disk to the most distant point of the colony. The previously described formula was used to determine the growth rate (Guigón-López *et al*., 2010). In the PDA and SNA media, the color and edge of the colony were evaluated, whereas in CMA, pustule size, type of development, shape of the conidiophores, the position of the chlamydospore, and shape and size of the phialides and conidia were determined. The structures were mounted on slides using the adhesive tape and glycerin technique (Gary and Prakash, 2015) and observed under a compound microscope with a 100x lens (Carl Zeiss®; Axio Imager M2, Germany). The shape and size (µm) of 30 phialides and 30 conidia were recorded for each isolate.

Molecular identification of *S. rolfsii* and *Trichoderma* spp. Three disks of each isolate were placed in centrifuge tubes containing 25 mL of nutrient broth. The cultures were incubated at 27 °C and constantly shaken for five days at 150 rpm (Labnet International, Inc.®; Labnet Incubator Shaker 311DS, USA). The mycelium was placed in 2 mL Eppendorf tubes. The genomic DNA was obtained with the CTAB method at 2% (Sanger *et al*., 1977) and finally adjusted to 50 ng µL^{-1}. The presence and integrity of the genomic DNA was verified by electrophoresis (Thermo Scientific®; Electrophoresis Power Supply EC1000XL, China) in 1% agarose gel 1%. The bands were observed using a photodocumentation system (BIORAD®; Universal Hood ll, USA). The DNA concentration and quality was determined in a NanoDrop (Thermo Scientific®; NanoDrop One ND-ONE, USA).

The molecular identification of the *Sclerotium* isolates was carried out with the Polymerase Chain Reaction (PCR) to amplify a fragment of 670 ± pb of the Internal Transcribed Spacer (ITS) with oligonucleotides ITS1 (5´ TCC GTA GGT GAA CCT TGC GG 3´) and ITS4 (5´ TCC TCC GCT TAT TGA TAT GC 3´) (White *et al*., 1990). Oligonucleotides fRPB2-5F (5' GAT CGA TCA CGA TGA TCA TCT TTC GG 3') and fRPB2-7cR (5' CCC ATA GGC TTG TCT TAG CCC AT 3') (Liu *et al*., 1999) were used to amplify a 1100 ± pb fragment of the subunit of polymerase II RNA (RPB2) from *Trichoderma* (Chaverril *et al*., 2003). The reaction mixture for each sample was 25 µL, which contained 1X buffer, 0.2 µg µL^{-1} BSA, 0.2 mM dNTP´s, 1.5 mM MgCl2, 0.5 µM of each oligonucleotide, 0.1 U µL^{-1} of Taq polymerase (Promega®) and 50 ng of ADN. The final volume was adjusted with ultrapure water. The conditions of amplification were as follows: initial 94 °C denaturation for 5 min, 35 denaturation cycles at 94 °C for 30 seg, alignment (57 °C for ITS and 54 °C for RPB2) for 40 sec and a 72 °C extension for 45 seg, followed by a final extension at 72 °C for 5 min in a thermocycler (BIORAD®; C1000 Thermal Cycler CFX96, Singapore). A total of 5 µL of reaction product and 1X loading buffer (Promega®) were used to perform electrophoresis in 1.5% agarose gel. The amplified fragments were observed using the photodocumentation system and sent for sequencing to Macrogen® Seoul, Korea.

The sequences of the ITS region for *S. rolfsii* and the RPB2 gene for *Trichoderma* were edited in the BioEdit program, version 7.2.5 (Hall, 1999) and compared in the GenBank data base, using the BLASTn algorithm. The sequences obtained were aligned with reference sequences, belonging to types strains of different species within the *Trichoderma* complexes (*T. harzianum* and *T. viride*), as well as type strains belonging to *Sclerotium rolfsii*, using the MUSCLE software (Edgar, 2004) implemented in MEGA X, version 10.2.4 (Kumar *et al*., 2018). The *Ceratobasidium cornigerum* (AJ302006) and *Protocrea pallida* (CBS 121552) sequences were used as an external group in the phylogenetic analysis of *Sclerotium* and *Trichoderma*, respectively. The alignment underwent a model-fit test for nucleotide substitution and partitioning scheme in PartitionFinder v1.1.1 (Lanfear *et al*., 2012), following the greedy algorithm and the Akaike Information Criterion (AIC). Phylogenetic inference for *Trichoderma* was carried out by Maximum Likelihood (ML) in RAxML v7.2.8 (Stamatakis, 2006) and Bayesian Inference (BI) in MrBayes 3.2.7 (Ronquist *et al.,* 2012), whereas inference for *Sclerotium* was performed only by ML. In both analyses, the General Time Reversible model with gamma distribution and invariant sites (GTRGAMMAI) and the partitioning scheme defined by PartitionFinder were used. The ML analysis used 1,000 bootstrap replicates, and BI used 2 simultaneous runs of 1 million generations with six Markov and Monte Carlo chains, sampling every 1,000 trees and discarding 20% of trees as burn-in. Run stability and convergence were evaluated in Tracer ver. 1.7.2 (Rambaut *et al.,* 2018). Phylograms were edited in FigTree v1.4.0 (Rambaut, 2014).

Pathogenicity of *Sclerotium rolfsii* in potato tubers. The pathogenicity of 20 *S. rolfsii* isolates (Scr2, Scr3, Scr4, Scr5, Scr6, Scr7, Scr8, Scr9, Scr10, Scr11, Scr12, Scr13, Scr14, Scr17, Scr47, Scr48, Scr49, Scr50, Scr51 and Scr54), obtained from soils that had undergone potato plantation in Sonora and Sinaloa was evaluated. Potato tubers var. Fianna were superficially washed and disinfected with 70% alcohol. Five healthy tubers were used for each treatment and placed in moist chambers to achieve high relative humidity. A superficial lesion was created in the tuber with a hole puncher, 5 mm in diameter, and on the lesion, a PDA disk, 5 mm in diameter, was placed with active fungal growth. As a control, tubers were inoculated with PDA disks without the fungus. The inoculated tubers and controls were placed in a bioclimatic chamber at 27 °C (Daami-Remadi *et al.,* 2012).

The data for temperature and moisture inside the moist chamber were recorded with a MadgeTech®; RFRHTemp2000A, Wireless Temperature / Humidity Data Logger, USA once per hour during the experiment.

The pathogenicity and virulence of the isolates in the tubers was determined eight days after the inoculation with the pathogen; for this, the tubers were cut transversally in the center of the lesion and the maximum width (W) and depth (PR) of the lesion were measured to determine the penetration of the pathogen (P), which was calculated using the formula by Lapwood *et al*. (1984): $P\ (mm) = (A / 2 + (PR - 6)) / 2$. The percentage of soft rot of the tuber tissues was also estimated, using the methodology by Bourne *et al*. (1981) and Hildenbrand and Ninnemann (1994), which consists of weighing each tuber (PT), then extracting the damaged (rotten) tissue and weighing again (PS). To determine the percentage of tissue with rotting, the following formula was used: $(\%) = (PT - PS / PT) \times 100$. Subsequently, the pathogen was isolated from the tissue that displayed characteristic symptoms of the disease, and it was morphologically identified to fulfill Koch's postulates. The experiment was run twice.

Statistical data analysis. The normality of the data on the penetration and percentage of soft rot caused by the pathogen was verified using the Kolmogorov-Smirnov test with the SAS 9.0 statistical package. The analyses showed that the data distribution was not normal, therefore the data was subject to a non-parametric Kruskal-Wallis analysis with a value of ($P>0.05$).

RESULTS AND DISCUSSION

Population density, isolation and morphological characterization of *S. rolfsii isolates*. Twenty *S. rolfsii* isolates were obtained from the same number of fields, during the time of sampling of the 239 plots from Sonora and Sinaloa, which accounted for 8.4% of the plots in which the fungus was found; the population density varied between 2 and 24 sclerotia per kg of soil (Table 1). The isolates presented whitish mycelia with a fibrous and cottonlike appearance, and fan-shaped (Figure 1A). Hialin hyphae, septated, with fibulae (Figure 1B). Shades ranging from whitish to yellowish were reported on the reverse side of the colonies, similar to what was reported by Paparu *et al.* (2020). According to Mahadevakumar *et al.* (2018) *S. rolfsii* presents different morphological characteristics, in both its colony and in the sclerotia, influenced by the wide range of hosts and weather conditions in which it develops.

The isolates displayed a radial growth of 4-16 mm/day, until they reached a diameter of 90 mm in the Petri dish, between 5 and 8 days of incubation (Prasad *et al.*, 2012). Okereke and Wokocha (2007) reported that the variation in the growth of the isolates is due to differences in the levels of nutrients, ecology or genetic differences.

The sclerotia developed 10 to 20 days after transferring the isolates to the medium in Petri plates, and their diameter varied, between 0.5 and 2 mm. The isolates formed between 18 and 153 sclerotia per Petri dish. The sclerotia displayed a light maroon to dark maroon color, depending on their level of maturation, similar to the morphological structures published by Zhou *et al.* (2019). Likewise, the size of the sclerotia was similar to those a lo reported by Díaz-Nájera *et al.* (2018).

Table 1. Identification, population density and origin of 20 *S. rolfsii* isolates obtained from soils in which potato is grown in Sonora and Sinaloa.

Code	Identification	Esclerotia/kg of soil	Growing season	Municipality/State	Coordenates	GenBank code
Scr2	*S. rolfsii*	8	2019-2020	El Fuerte, Sinaloa	25.9425 -108.809166	OR514111
Scr3	*S. rolfsii*	10	2019-2020	Ahome, Sinaloa	25.7775 -109.040277	OR514112
Scr4	*S. rolfsii*	24	2019-2020	Ahome, Sinaloa	25.701944 -109.043333	OR514113
Scr5	*S. rolfsii*	6	2019-2020	Ahome, Sinaloa	25.851944 -108.885	OR514114
Scr6	*S. rolfsii*	12	2019-2020	Ahome, Sinaloa	25.669722 -109.006111	OR514115
Scr7	*S. rolfsii*	10	2019-2020	Ahome, Sinaloa	25.769444 -109.045	OR514116
Scr8	*S. rolfsii*	20	2019-2020	Ahome, Sinaloa	25.836944 -108.926388	OR514117
Scr9	*S. rolfsii*	4	2019-2020	Ahome, Sinaloa	25.691944 -109.010277	OR514118
Scr10	*S. rolfsii*	6	2019-2020	El Fuerte, Sinaloa	25.9449166 -108.908333	OR514119
Scr11	*S. rolfsii*	2	2019-2020	Ahome, Sinaloa	25.743611 - 108.998611	OR514120
Scr12	*S. rolfsii*	4	2019-2020	Ahome, Sinaloa	25.876111 -108.835	OR514121
Scr13	*S. rolfsii*	2	2019-2020	Guasave, Sinaloa	25.6525 -108.763888	OR514122
Scr14	*S. rolfsii*	8	2019-2020	Ahome, Sinaloa	25.789166 -108.895277	OR514123
Scr17	*S. rolfsii*	18	2019-2020	Ahome, Sinaloa	25.77333 -109.280277	OR514124
Scr47	*S. rolfsii*	2	2021-2022	Ahome, Sinaloa	25.465355-108.542845	OR514125
Scr48	*S. rolfsii*	6	2021-2022	Ahome, Sinaloa	25.464949 -108.543231	OR514126
Scr49	*S. rolfsii*	16	2021-2022	Ahome, Sinaloa	25.465739 -108.541982	OR514127
Scr50	*S. rolfsii*	10	2021-2022	Ahome, Sinaloa	25.465119 -108.543142	OR514128
Scr51	*S. rolfsii*	14	2021-2022	Ahome, Sinaloa	25.464987 -108.543004	OR514129
Scr54	*S. rolfsii*	18	2021-2022	Altar, Sonora	30.9451630 -111.8302930	OR514130

Regarding the production of sclerotia, the results of this study are consistent with those reported by Ayed *et al*. (2018); their formation began in the same period recorded by Mahadevakumar *et al*. (2018). This differs from what was documented by Paparu *et al*. (2020), who reported the production of sclerotia 28 days after growth on PDA.

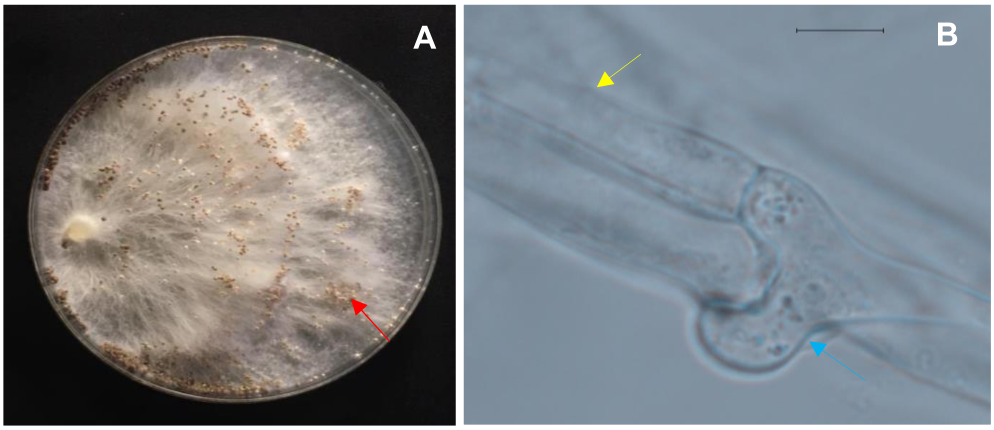

Figure 1. Morphological characteristics of Sclerotium rolfsii (Scr17). (**A**) Colony morphology in PDA medium, and sclerotia (red arrow); (**B**) Hyphal hyalin (yellow arrow) and fibulae (blue arrow) (100x). Scale: (B= 50 µm).

The Maximum Likelihood dendrogram generated with *Sclerotium* ITS region sequences showed that the 20 isolates obtained from 20/239 potato fields is shown on Figure 2.

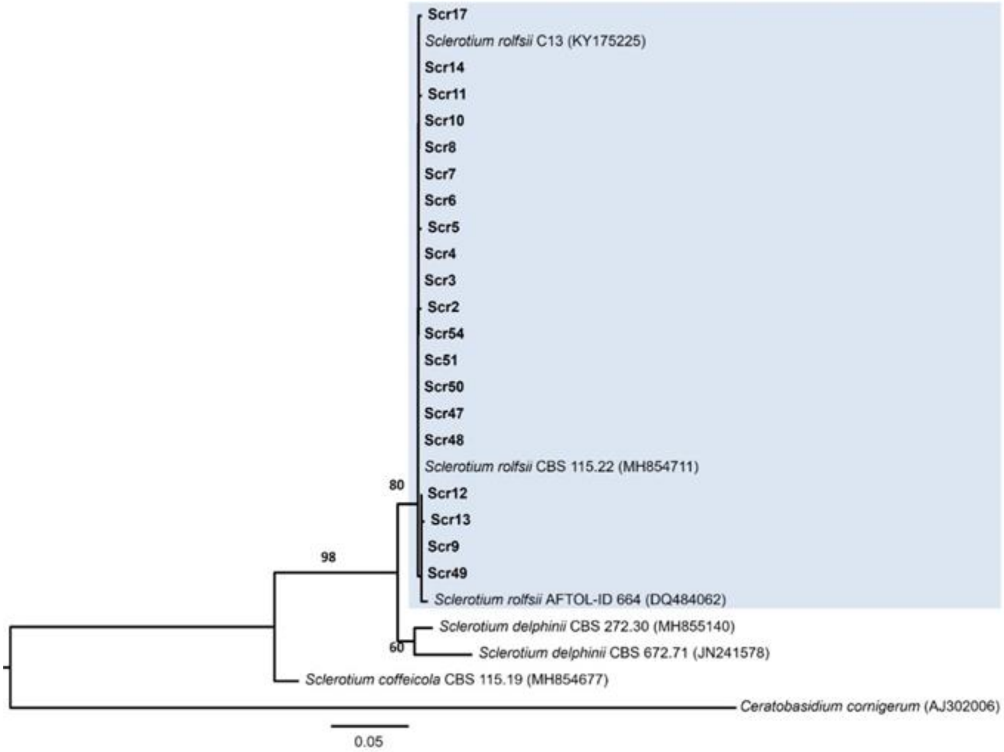

Figure 2. Phylogenetic analysis of *Sclerotium rolfsii* from Sonora and Sinaloa. Maximum likelihood tree based on the Internal Transcribed Spacer (ITS) of 20 *S. rolfsii* isolates. The isolates characterized in this study appear in bold letters. The bootstrap values over 50 are shown as percentages. The scale bar indicates the expected number of nucleotide substitutions.

The analysis showed that all 20 isolates: Scr2, Scr3, Scr4, Scr5, Scr6, Scr7, Scr8, Scr9, Scr10, Scr11, Scr12, Scr13, Scr14, Scr17, Scr47, Scr49, Scr49, Scr50, Scr51 and Scr54 belonged to the species *Sclerotium rolfsii*, as they clustered with the sequences of the type C13 (KY175225), CBS 115.22 (MH854711) and AFTOL-ID (DQ484062) isolates of this species, with a high bootstrap support (80%) (Figure 2); these results coincide with reports by Mahadevakumar *et al*. (2018).

Population density and morphological and molecular characterization of *Trichoderma* species isolates. Twenty-six *Trichoderma* spp. isolates were obtained from soil from 239 fields from Sonora and Sinaloa, which accounted for 10.9% of the plots with the fungus, with a population density of 2 to 8 Culture-Forming Units per gram of soil (UFC g^{-1}) (Table 2).

Table 2. Identification ID, population density (CFU) and origin of 26 *Trichoderma* isolates sampled from soil of potato (*S. tuberosum*) commercial fields in Sonora and Sinaloa.

Code	Species [x]	CFU g^{-1}	Growing season	Municipality/ State	Coordenates	GenBank code
TES19	*T. asperelloides*	4	2020-2021	Caborca, Sonora	31.041666 -112.331111	OR521159
TES20	*T. asperelloides*	2	2020-2021	Altar, Sonora	31.062222 -111.834722	OR521160
TAF21	*T. afroharzianum*	6	2020-2021	Altar, Sonora	30.909444 -111.804444	OR521161
TAM22	*T. asperellum*	4	2020-2021	Caborca, Sonora	30.541388 -112.273611	OR521162
TES23	*T. asperelloides*	8	2020-2021	Caborca, Sonora	31.995555- 112.360277	OR521163
TES24	*T. asperelloides*	6	2020-2021	Caborca, Sonora	31.066660- 112.338333	OR521164
TES26	*T. asperelloides*	4	2020-2021	Caborca, Sonora	30.660000 -111.270550	OR521165
TAM27	*T. asperellum*	2	2019-2020	Guasave, Sinaloa	25.722955 -108.740276	OR521166
TAM30	*T. asperellum*	2	2019-2020	El Fuerte, Sinaloa	25.944916 -108.908333	OR521167
TAM31	*T. asperellum*	2	2019-2020	Guasave, Sinaloa	25.655277 -108.561944	OR521168
TAF33	*T. afroharzianum*	4	2020-2021	S. de Leyva, Sin.	25.952500 -108.406388	OR521169
TAM35	*T. asperellum*	4	2020-2021	Ahome, Sinaloa	25.760550 -109.266388	OR521170
TAM37	*T. asperellum*	6	2020-2021	Guasave, Sinaloa	25.712500 -108.782222	OR521171
TAF38	*T. afroharzianum*	8	2020-2021	Guasave, Sinaloa	25.580833 -108.603055	OR521172
TAM57	*T. asperellum*	8	2021-2022	Ahome, Sinaloa	25.481112 -108.571717	OR521173
TAM59	*T. asperellum*	6	2021-2022	Guasave, Sinaloa	25.679176 -108.665316	OR521174
TAM64	*T. asperellum*	4	2021-2022	Ahome, Sinaloa	25.819266 -108.955429	OR521175
TES65	*T. asperelloides*	4	2021-2022	Ahome, Sinaloa	25.491132 -108.571830	OR521176
TAM67	*T. asperellum*	2	2021-2022	Ahome, Sinaloa	25.491299 -108.571854	OR521177
TAM68	*T. asperellum*	2	2021-2022	Ahome, Sinaloa	25.491496 -108.571569	OR521178
TAM69	*T. asperellum*	2	2021-2022	Ahome, Sinaloa	25.491299 -108.571854	OR521179
TAM70	*T. asperellum*	4	2021-2022	Ahome, Sinaloa	25.498320 -108.571704	OR521180
TAI73	*T. azevedoi*	2	2021-2022	Ahome, Sinaloa	25.498320 -108.572148	OR521181
TAM74	*T. asperellum*	4	2021-2022	Ahome, Sinaloa	25.491445 -108.571659	OR521182
TAF75	*T. afroharzianum*	4	2021-2022	Ahome, Sinaloa	25.498320 -108.572148	OR521183
TAM76	*T. asperellum*	6	2020-2021	Caborca, Sonora	31.995555 -112.360277	OR521184

[x] Species were identified based on morphological and molecular characteristics.

Based on the morphological characteristics, it was determined that the *Trichoderma* isolates belonged to two species complexes: 21 isolates belonged to the *T. viride* complex (TES19, TES20, TAM22, TAM23, TES24, TES26, TAM27, TAM30, TAM31, TAM35, TAM37, TAM57, TAM59, TAM64, TES65, TAM67, TAM68, TAM69, TAM70, TAM74 and TAM76) (Table 3; Figure 3) and five, to the *T. harzianum* complex (TAF21, TAF33, TAF38, TAI73 y TAF75) (Table 3; Figure 4).

The isolates of the *T. viride* complex displayed a growth rate in PDA of 10-18 mm/day, and in SNA, of 8-14 mm/day (Table 3), similar what Guigón-López *et al*. (2010) reported. The colony morphology was similar for all isolates in CMA, where the color of the colony varied from light green to dark green as they matured. The edge was wavy and smooth, with a floccose to arachnoid appearance, aqueous white mycelium and hyaline hyphae (Table 3; Figure 3A y B) (Rai *et al*., 2019). Dark green pustules, 1-2 mm in diameter (Table 3; Figure 3C). Long and branched conidiophores (Table 3; Figure 3D and E). Sub-globose to globose, smooth conidia, 2.5 to 3.8 µm long and 2.0 to 3.0 µm wide (Table 3; Figure 3F). Lageniform-thin phialides with branched ends, 4.2 to 14.3 µm long and 2.6 to 5.0 µm wide (Table 3; Figure 3D y E). No chlamidospores were found (Table 3) (Gary and Prakash, 2015).

On the other hand, the *T. harzianum* complex isolates displayed a growth rate of 11 to 19 mm/day in PDA and 11 to 17 mm/day^{-} in SNA (Table 3; Figure 4A and B), which coincides with the ranges reported by Gary and Prakash, (2015). In HMA, the pustules were light green in color (Table 3; Figure 4C) (Rai *et al*., 2019), with sub-globose, smooth conidia, 2.0 to 3.0 µm long and 1.6 to 2.3 µm wide (Table 3; Figure 4H). Ampulliform phialides with a distinctive neck and a narrow tip, 5.8 to 7.2 µm long and 2.5 to 3.0 µm wide (Table 3; Figure 4F and G). Intercalary and terminal chlamydospores were observed (Table 3; Figure 4D and E) (Gary and Prakash, 2015).

Table 3. Morphological characteristics of isolates of the *Trichoderma viride* and *Trichoderma harzianum* species complexes in three culture media.

Morphological characteristics[Z]		**Culture medium**	***T. viride***	***T. harzianum***
Colony	Radial mycelial growth (mm/day)	PDA	10 - 18	11 - 19
		SNA	8 - 14	11 - 17
	Color	PDA SNA CMA	Light green to dark green	Light green to dark green
Pustules	Size(mm)	CMA	1 - 2	1 - 2
Mycelium	Shape	PDA and CMA	Floccosase and arachnoid	Floccosase and arachnoid
	Hyfae color		Hyaline	Hyaline
Conidium	Shape	CMA	Subglobose, ovoid, Smooth, warty	Subglobose, Smooth
	Size (length)		2.47-3.78 µm	2.03-2.99 µm
	Size (width)		2.02-3.05 µm	1.64-2.30 µm
Conidiophores	Shape	CMA	Long and branched	Branched
Chlamidospores	Position	CMA	**Absent**	**Terminal and intercalar**
Phialides	Shape	CMA	**Lageniform and thin**	**Ampuliform**
	Size (Length)		4.2-14.3 µm	5.8-7.2 µm
	Size (width)		2.6-5.0 µm	2.5-3.0 µm

[Z] The morphological characteristics were determined in 2- to 3-day old colonies with 12-hour light regimes. In bold the characteristics are more distinctive.

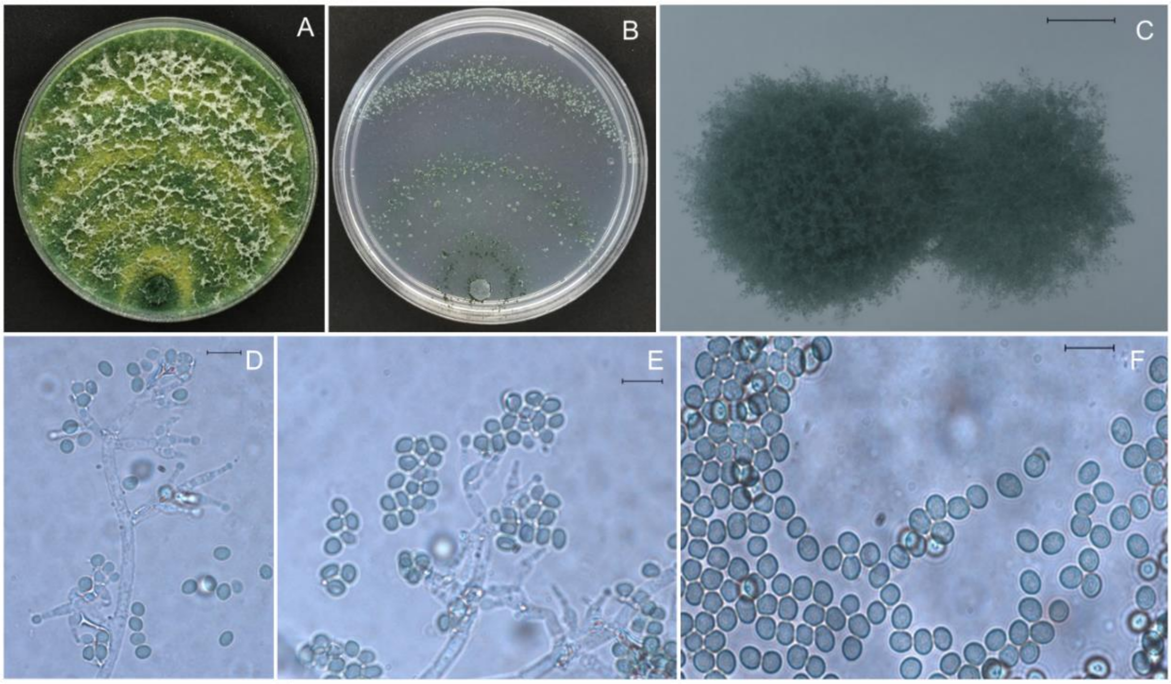

Figure 3. Colony and microscopic morphology of *Trichoderma asperellum* (TES19). (**A**) colony in PDA culture medium. (**B**) colony in SNA culture medium. (**C**) conidial pustules. (**D** and **E**) conidiophores and (**F**) conidia (100x). (**C-F**) in HMA medium. Scale: (C= 2 mm) (D= 10 µm) (E and F= 5 µm). This species belongs to *T. viride* complex.

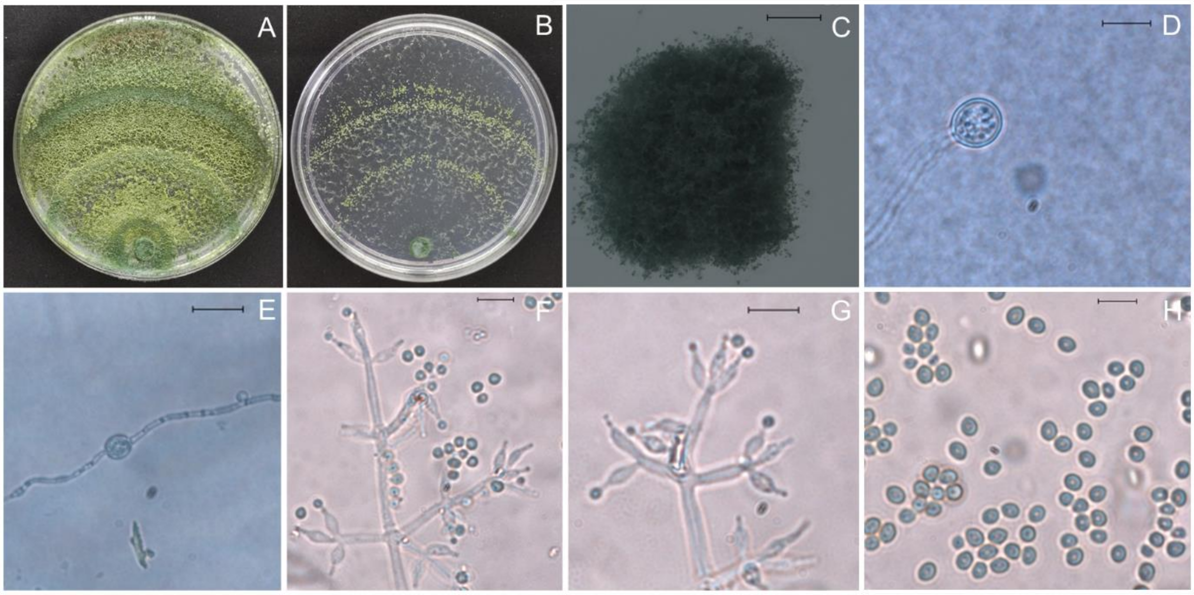

Figure 4. Colony and microscopic morphology of *Trichoderma afroharzianum* (TAF33). (**A**) colony in PDA culture medium. (**B**) colony in SNA culture medium. (**C**) conidial pustules. (**D and E**) chlamidospores and (**F and G**) conidiophores (**H**) conidia (100x). (C-H) in HMA medium. Scale: (C= 2 mm) (D and H= 5 µm) (E, F and G= 10 µm). This species belongs to *T. harzianum* complex.

The Maximum Likelihood dendrogram of the RPB2 gene for the *T. viride* complex identified two species among the 16 analyzed isolates. Isolates TAM76, TAM67, TAM30, TAM35, TAM37, TAM57, TAM23, TAM59, TAM27, TAM69, TAM22, TAM31, TAM70, TAM68, TAM64 and TAM74 were clustered with the sequences from strains GJS 01-15, TR3(T) and GJS 02-63 of *Trichoderma asperellum*¸ with a bootstrap support of 78% and a 0.99 PP, whereas isolates TES19, TES20, TES26, TES24 and TES65 were clustered with strains GJS 02-63, GJS 04-111(T) and CML 2676 of *Trichoderma asperelloides*

(Bootstrap 98%; PP 1; Figure 5). On the other hand, the phylogram of the *T. harzianum* complex confirmed that isolates TAF21, TAF38, TAF75 and TAF33 belonged to the species *Trichoderma afroharzianum*, since they are clustered with the sequences of the strain of this species, CEN1417, CEN1410, GJS 04-186(T) and CBS 466.94, with a high bootstrap support (92%) and a posterior probability (1). On the other hand, isolate TAI73 was identified as *Trichoderma azevedoi*, since it formed a clade with the strains of this species, CEN1423, CEN1403 y CEN1422(T) (Bootstrap 53% and PP 0.72) (Figure 6). Jaklitsch and Voglmayr (2015) and Athafah *et al*. (2020) reported three *Trichoderma* species based on the region RPB2 (*T. asperellum, T. asperelloides* and *T. afroharzianum*) obtaining plant materials from forest areas. In turn, Inglis *et al*. (2020) identified *T. azevedoi* with the same region, in soil samples gathered from garlic and onion fields in eight different locations in Brazil.

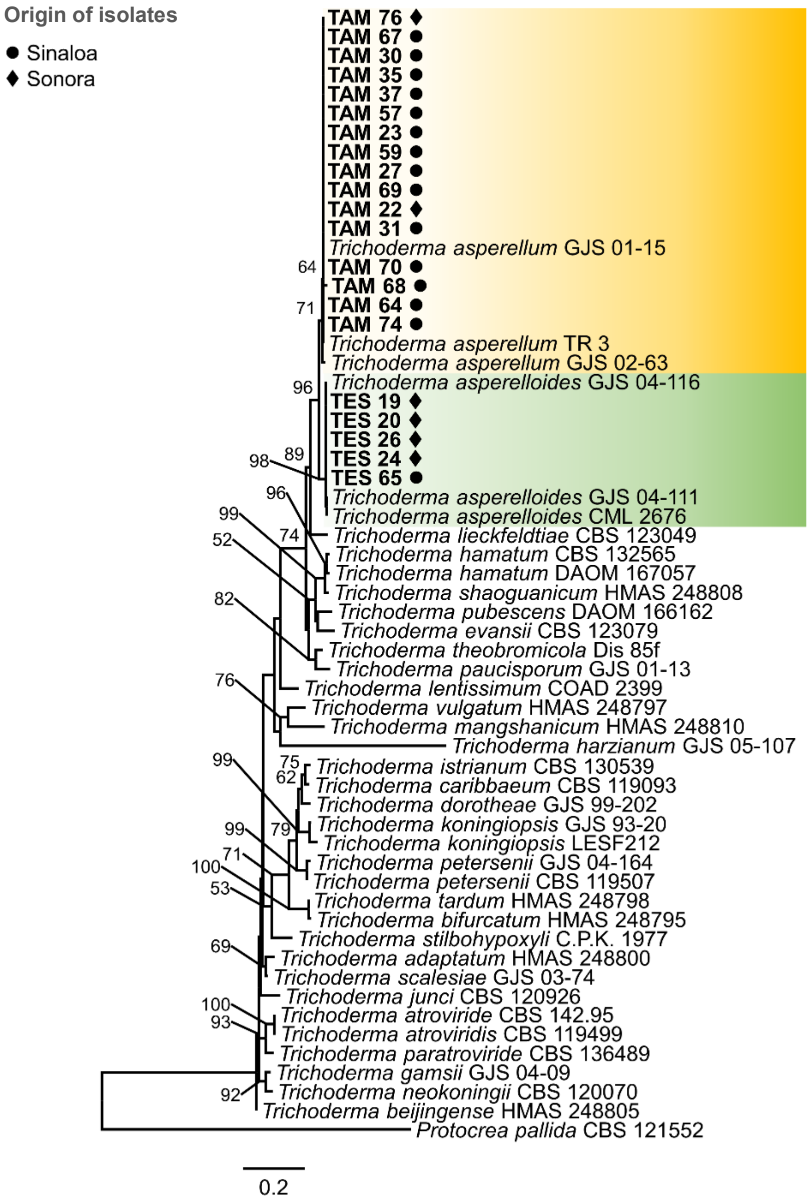

Figure 5. Maximum Likelihood phylogram of the *Trichoderma viride* species complex, based on the RNA polymerase II subunit (RPB2). The 21 *Trichoderma* isolates, obtained from potato plantations in Sonora and Sinaloa characterized in this study, appear in bold and highlighted in color. The bootstrap values >50 and the posterior probability values >0.5 are shown in the nodes. The scale bar indicates the expected number of nucleotide substitutions.

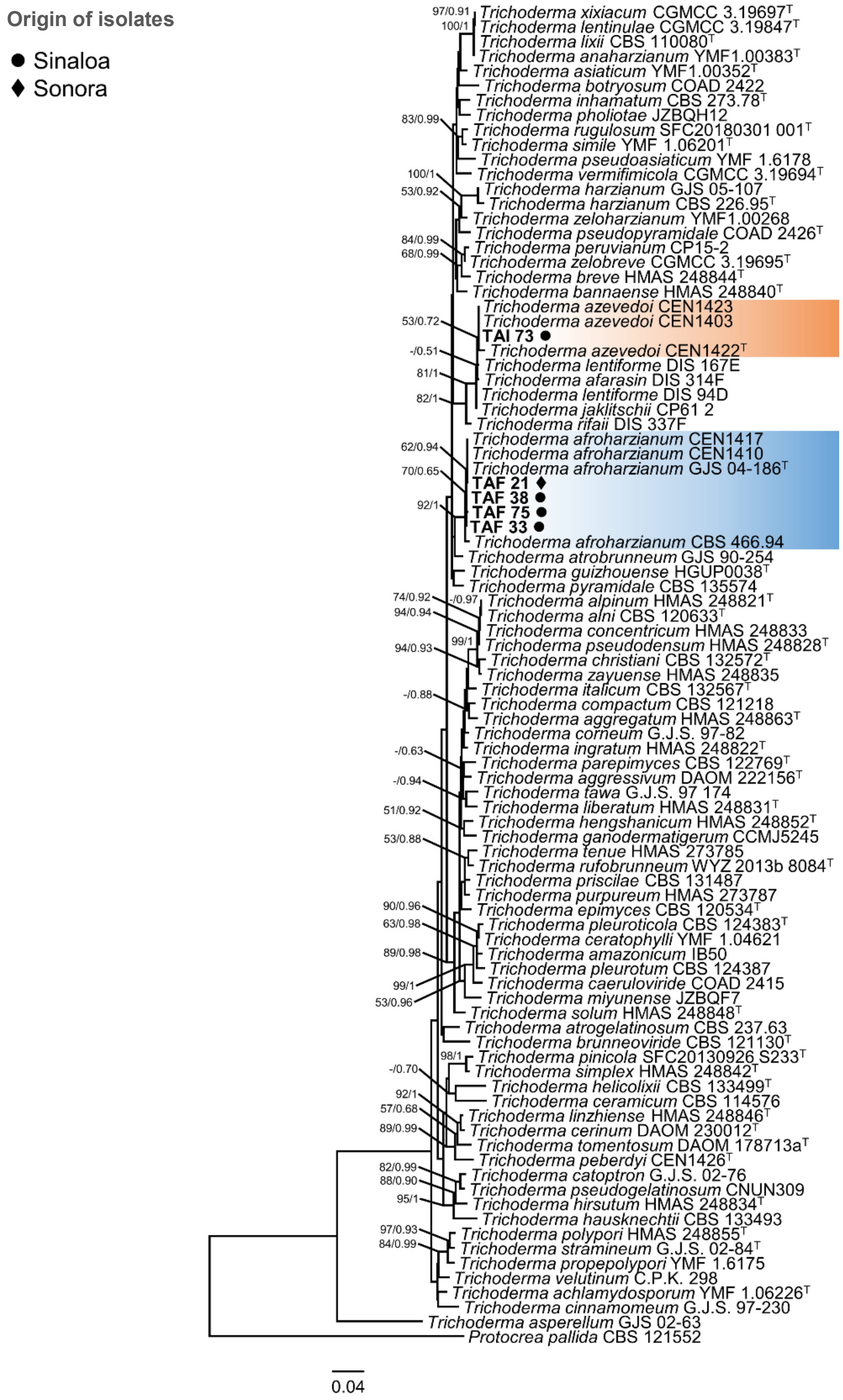

Figure 6. Maximum Likelihood phylogram of the *Trichoderma harzianum* species complex, based on the RNA polymerase II subunit (RPB2). The five *Trichoderma* isolates obtained from potato plantations in Sonora and Sinaloa characterized in this study, appear in bold and highlighted in color. The bootstrap values >50 and the posterior probability values >0.5 are shown in the nodes. The scale bar indicates the expected number of nucleotide substitutions.

Pathogenicity of *Sclerotium rolfsii* in potato tubers. Eight days after inoculation, all potato tubers of the Fianna variety inoculated with the *S. rolfsii* isolates displayed symptoms of soft rot (Paparu *et al.,* 2020; Paul *et al.,* 2021) (Table 4) with variations in the levels of virulence between isolates; this piece of information is worth considering when evaluating the genetic resistance of potato to the disease. Symptoms were similar to the lesions produced by the fungus in the field. The tubers displayed circular and irregular soft rot, with a brown edge (Figure 7), whereas the control tubers remained healthy throughout the experimental period. The penetration of the 20 isolations in the tuber varied from 9.5 to 16.9 mm, with significant differences ($P > 0.05$). The greatest penetration took place with isolate Scr4 (16.9 mm), whereas isolate Scr9 displayed the lowest penetration (9.5 mm). Isolate Scr7 caused a penetration of 15.2 mm, and displayed no significant differences with isolates Scr17, Scr48 and Scr10, with a penetration of 14.0, 13.7 and 13.6 mm, respectively (Table 4). On the other hand, the percentages of rotting varied from 1.4% to 10.5% with significant differences ($P > 0.05$) between the isolates. The highest percentage of rot was caused by isolate Scr4 (10.5%) and the lowest, with isolate Scr9 (1.4%), which displayed no significant differences with isolates Scr3, Scr47 and Scr5 with percentages of 2.0%, 3.9% and 4.5% respectively, although there were such differences with the rest of the isolates ($P > 0.05$). Isolate Scr4 displayed no significant differences ($P > 0.05$) with isolates Scr7, Scr10, Scr17, Scr51 and Scr6 with percentages of 9.3%, 8.4%, 8.0%, 8.0% and 7.7%, respectively (Table 4). Symptoms and signs of the disease were observed, similar to those that occur in the field, which coincides with the results by Daami-Remadi *et al.* (2007) when they showed the pathogenicity of the fungus in var. Spunta potato.

Table 4. Penetration of the pathogen and percentage of soft rot in potato tubers var. Fianna with artificial inoculation.

Penetration of the pathogen(mm)			**Soft rot (%)**		
Isolate	**N**	**Mean^x**	**Isolate**	**N**	**Mean^x**
Control	10	0.0 a	Control	10	0.0 a
Scr9	10	9.5 ab	Scr9	10	1.4 ab
Scr3	10	10.0 ab	Scr3	10	2.0 abc
Scr49	10	11.0 abc	Scr47	10	3.9 abcd
Scr5	10	11.1 abc	Scr5	10	4.5 abcde
Scr13	10	11.1 abc	Scr13	10	4.5 bcde
Scr2	10	11.2 abcd	Scr12	10	5.1 cdef
Scr12	10	11.5 bcde	Scr8	10	5.3 defg
Scr8	10	12.2 cdef	Scr49	10	5.6 defg
Scr14	10	12.3 def	Scr2	10	6.0 efg
Scr50	10	12.4 def	Scr48	10	6.1 efgh
Scr47	10	12.6 efg	Scr14	10	6.2 fgh
Scr6	10	12.7 fg	Scr50	10	6.2 fghi
Scr11	10	12.8 fg	Scr11	10	7 ghij
Scr51	10	12.9 fg	Scr54	10	6.9 ghij
Scr54	10	13.2 fgh	Scr6	10	7.7 hijk
Scr10	10	13.6 ghi	Scr51	10	8.0 hijk
Scr48	10	13.7 ghi	Scr17	10	8.0 ijk
Scr17	10	14.0 ghi	Scr10	10	8.4 jk
Scr7	10	15.2 hi	Scr7	10	9.3 jk
Scr4	10	16.9 i	Scr4	10	10.5 k

^{x}Means with at least a common letter are not significantly different ($P > 0.05$), Kruskal-Wallis. N= Repetitions

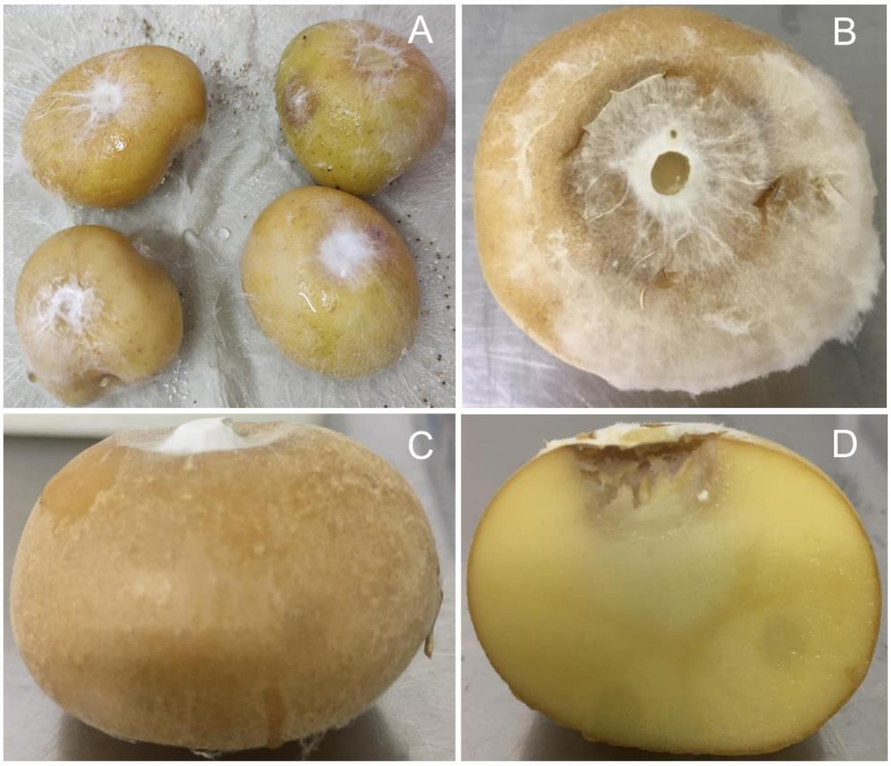

Figure 7. Symptoms of soft rot in Fianna variety potato tubers, caused by the isolate Scr17 of *S. rolfsii* by artificial inoculation. (**A**) Tubers with symptoms of *S. rolfsii* in a moist chamber. (**B and C**) lesions with cottonlike mycelium caused by the fungus. (**D**) Transverse cut of potato tuber with soft rot.

The results of this work are relevant because new lines of investigations are opened in which may include studies on the pathogenicity of *S. rolfsii* in different agricultural crops, crop rotation and its impact on the sclerotia populations, as well as the use of *Trichoderma* species on the reduction of sclerotia production and its correlation with the reduction of the incidence of the disease in the field. This is because *Trichoderma* has been identified as a promising biological control agent against soil pathogens such as *S. rolfsii* in the potato crop (Rubayet and Bhuiyan, 2016; Chowdhury *et al.,* 2023). The use of endemic *Trichoderma* species obtained from fields planted with potato where they have been exposed to the pressure of several fungicides, suggests that they have become resistant to these types of molecules. This implies that they could be used in combination with fungicides to which they are resistant, for the control of potato soft rot, as a strategy to reduce the doses of synthetic fungicides.

CONCLUSIONS

A total of 239 commercial potato plots were sampled in Sonora and Sinaloa during the 2019-2020, 2020-2021 and 2021-2022 agricultural cycles. Out of these plots, 8.4% were positive for *S. rolfsii,* with a population density of 2 to 24 sclerotia per kg of soil. The identity of the fungus was confirmed using conventional techniques and molecular tools. The capacity of *S. rolfsii* to induce soft rot in Fianna variety potato tubers was confirmed, with a variation in the virulence between isolates. The penetration of the pathogen fluctuated between 9.5 and 16.9 mm, whereas the percentage of rot varied from 1.4 to 10.5%, with isolate Scr4 standing out as the most aggressive.

On the other hand, 26 *Trichoderma* spp. isolates were obtained, accounting for 10.9% of the plots in which the fungus was located, with a population density of 2 to 8 UFC g^{-1} of soil. Morphological and molecular characterization enabled the identification of *T. asperellum*, *T. asperelloides*, *T. afroharzianum* and *T. azevedoi*, which belong to the *T. viride* and *T. harzianum* complexes.

The findings of this work have significant implications for the management of soft rot in potato tubers. The identification of native *Trichoderma* species with antagonistic potential opens future lines of investigation related to the implementation of biological control strategies, particularly in systems in which resistance to fungicides is a limitation. In addition, the variability in the virulence of *S. rolfsii* suggests the need for additional studies to understand their interaction with the host and the environment, as well as to develop cultural practices that reduce the survival of sclerotia in the soil.

Limitations. This paper did not include *Trichoderma* and *S. rolfsii* confrontation tests.

Conflict of interest. None to be reported.

Funding. UAO and Local SV Board, Valle del Fuerte.

Acknowledgements. The authors would like to thank the potato farmers in Sinaloa and Sonora for their disposition towards this investigation.

Contribution of authors. The first four authors contributed with lab, analysis and interpretation work. The second author was responsible for the experimental conception, writing and revision of the manuscript. The fifth and sixth authors were in charge of field management sampling.

REFERENCES

Armenta-López SE, Valenzuela-Solano C and Hernández-Martínez R. 2021. Identification and molecular analysis of races of *Fusarium oxysporum* f. sp. *lycopersici* isolated from tomato in Baja California, Mexico. Revista Mexicana de Fitopatología 39:266-288. https://doi.org/10.18781/r.mex.fit.2103-4

Athafah AT, Sabah IAA, Li B and Jing-Ze Z. 2020. A new species of *Trichoderma* and gliotoxin role: A new observation in enhancing biocontrol potential of *T. virens* against *Phytophthora capsici* on chili pepper. Biological Control 145:1-11. https://doi.org/10.1016/j.biocontrol.2020.104261

Aycock R. 1966. Stem rot and other diseases caused by *Sclerotium rolfsii* or the status of Rolf's fungus after 70 years. North Carolina Agricultural Experiment Station Technical Bulletin. Editor North Carolina Agricultural Experiment Station 174:202.

Ayed F, Jabnoun KH, Aydi B, Abdallah R and Daami RM. 2018. Effect of temperatures and culture media on *Sclerotium rolfsii* mycelial growth, sclerotial formation and germination. Journal of Plant Pathology and Microbiology 9:1-9. https://doi.org/10.4172/2157-7471.1000446

Bourne WF, McCalmont DC and Wastie RL. 1981. Assessing potato tubers for susceptibility to bacterial soft rot (*Erwinia carotovora* subsp. *atroseptica*). Potato Research. 24:409-415. https://doi.org/10.1007/BF02357323

Browne WR, DeTar B and Sanden CJ. 2002. Phene Comparison of drip and sprinkler irrigation systems for applying metam sodium and managing stem rot on potato. Plant Disease 86:1211-1218. https://doi.org/10.1094/PDIS.2002.86.11.1211

Chaverri P, Castlebury LA, Overton BE and Samuels GJ. 2003. *Hypocrea/Trichoderma*: species with conidiophore elongations and green conidia. Mycologia 95:1100-1140. https://doi.org/10.1080/15572536.2004.11833023

Chowdhury Md.R, Ahmed SF, Khalid B, Ferdaous BZ, Ferdoushi AJ, *et al*. 2023. Biocontrol efficiency of microencapsulated *Trichoderma harzianum* coupled with organic additives against potato stem rot caused by *Sclerotium rolfsii*. Plant Stress 9:1-9 https://doi.org/10.1016/j.stress.2023.100181

Daami-Remadi M, Jabnoun-Khiareddine H, Ayed F, Hibar K and Mahjoub M. 2007. First report of *Sclerotium rolfsii* causing atypical soft rot on potato tubers in Tunisia. Tunisian Journal of Plant Protection 2:59-62. https://www.researchgate.net/publication/265427357

Daami-Remadi M, Jabnoun-Khiareddine H, Sdiri A and El Mahjoub M. 2012. Comparative reaction of potato cultivars to *Sclerotium rolfsii* assessed by stem rot and tuber decay severity. Pest Technology 6: 54-59. https://www.researchgate.net/publication/311651863_Comparative_Reaction_of_Potato_Cultivars_to_Sclerotium_rolfsii_Assessed_by_Stem_Rot_and_Tuber_Decay_Severity

Díaz-Nájera JF, Sahagún-Castellanos J, Vargas-Hernández M, Ayvar-Serna S, Alvarado-Gómez OG, *et al*. 2018. Diagnosis and integrated management of fruit rot in *Cucurbita argyrosperma*, caused by *Sclerotium rolfsii.* Plant Pathology Journal 34:171–181. https://doi.org/10.5423/PPJ.OA.08.2017.0185

Edgar RC. 2004. MUSCLE: multiple sequence alignment with high accuracy and high throughput. Nucleic Acids Research 32:1792-1797. https://doi.org/10.1093/nar/gkh340

Estrada VMN, Vélez APE y López NJC. 1997. Estandarización de una metodología para obtener cultivos monospóricos del hongo *Beauveria bassiana.* Cenicafé 48:59-65.

Fiers M, Edel-Hermann V, Chatot C, Le-Hingrat Y, Alabouvette C, *et al*. 2012. A review. Agronomy for Sustainable Development. Potato soil-borne diseases 32:93-132. https://doi.org/10.1007/s13593-011-0035-z

Food Agricultural Organization of The United Nations (FAO). 2024. International Day of Potato: At inaugural celebration, FAO highlights crop’s significance and further potential. https://www.fao.org/newsroom/detail/international-day-of-potato--at-inaugural-celebration--fao-highlights-crop-s-significance-and-further-potential/en

García-González J, Mehl HL, Langston DB and Rideout SL. 2022. Planting date and cultivar selection to manage southern blight in potatoes in the mid-Atlantic United States. Crop Protection 162:1-8. https://doi.org/10.1016/j.cropro.2022.106077

Garibaldi A, Gilardi G and Gullino ML. 2007. First Report of Southern Blight Incited by *Sclerotium rolfsii* on Potato (*Solanum tuberosum*) in Northern Italy. The American Phytopathological Society 90:1114. https://doi.org/10.1094/PD-90-1114C

Gary JS and Prakash KH. 2015. *Trichoderma:* Identification and Agricultural Applications. The American Phytopathological Society. USA. 196p.

Guigón-López C, Guerrero–Prieto V, Vargas–Albores F, Carvajal–Millán E, Ávila–Quezada GD, *et al*. 2010. Identificación molecular de cepas nativas de *Trichoderma* spp. su tasa de crecimiento *in vitro* y antagonismo contra hongos fitopatógenos. Revista Mexicana de Fitopatología 28:87-96. versión On-line ISSN 2007-8080 versión impresa ISSN 0185-3309. https://www.redalyc.org/articulo.oa?id=61218468002

Guzmán VP, Bravo LL, Montes BR, Guigón LC and Sepúlveda JG. 2014. Induction of resistance to *Sclerotium rolfsii* in different varieties of onion by inoculation with *Trichoderma asperellum.* European Journal of Plant Pathology 138:223-229. https://doi.org/10.1007/s10658-013-0336-y

Haque S and Khan AA. 1977. A study of the differences in susceptibility of some potato varieties to *Sclerotium* wilt. Journal of the Bangladesh Agricultural Sciences 1:89-92.

Hall TA. 1999. BioEdit: a user-friendly biological sequence alignment editor and analysis program for Windows 95/98/NT. Nucleic Acids Symposium. Series. 41:95-98.

Herrera JE y Scott GJ. 1993. Factores limitantes a la producción y usos de la papa: resultados de la encuesta a los programas nacionales de América Latina. Revista Latinoamericana de La Papa. 5/6:122-134. https://www.researchgate.net/publication/267808125_Factores_limitantes_a_la_produccion_y_uso_de_la_papa_resultados_de_la_encuesta_a_los_programas_nacionales_de_america_latina

Hildenbrand S and Ninnemann H. 1994. Kinetics of phytoalexin accumulation in potato tubers of different genotypes infected with Erwinia carotovora ssp. Atroseptic. Physiological and Molecular Plant Pathology 44:335-347. https://doi.org/10.1016/S0885-5765(05)80047-5

Inglis PW, Mello SCM, Martins I, Silva JBT, Macêdo K, *et al*. 2020. *Trichoderma* from Brazilian garlic and onion crop soils and description of two new species: *Trichoderma azevedoi* and *Trichoderma peberdyi.* PLoS ONE 15:1-23. https://doi.org/10.1371/journal.pone.0228485

Jaklitsch WM and Voglmayr H. 2015. Biodiversity of *Trichoderma* (Hypocreaceae) in Southern Europe and Macaronesia. Publisher: Westerdijk Fungal Biodiversity Institute. Studies in Mycology 80:1-87. http://dx.doi.org/10.1016/j.simyco.2014.11.001

Kumar S, Stecher G, Li M, Knyaz C y Tamura K. 2018. MEGA X: Análisis de genética evolutiva molecular en plataformas informáticas. Biología Molecular y Evolución 35:1547-1549. https://doi.org/10.1093/molbev/msy096

Lanfear R, Calcott B, Ho S and Guindon S. 2012. PartitionFinder: combined selection of partitioning schemes and substitution models for phylogenetic analyses. Molecular Biology and Evolution 29:1695-1701. https://doi.org/10.1093/molbev/mss020

Lapwood DH, Read PJ and Spokes J. 1984. Methods for assesing the susceptibility of potato tubers of different cultivars to rotting by *Erwinia carotovora* subsp. a*troseptica* and *carotovora.* Plant Pathology 33:13-20. https://doi.org/10.1111/j.1365-3059.1984.tb00581.x

Liu YJ, Whelen S and Hall BD. 1999. Phylogenetic relationships among ascomycetes: evidence from an RNA polymerase II Subunit. Molecular Biology and Evolution 16:1799-1808. https://doi.org/10.1093/oxfordjournals.molbev.a026092

Mahadevakumar S, Chandana C, Deepika YS, Sumashri KS, Vandana Y, *et al*. 2018. Pathological studies on the southern blight of China aster (*Callistephus chinensis*) caused by *Sclerotium rolfsii.* European Journal of Plant Pathology 151:1081-1087. https://doi.org/10.1007/s10658-017-1415-2

Martínez-Martínez TO, Guerrero-Aguilar BZ, Pecina-Quintero V, Rivas-Valencia P, González-Pérez E, *et al*. 2020. Antagonismo de *Trichoderma harzianum* contra la fusariosis del garbanzo y su efecto biofertilizante. Revista Mexicana de Ciencias Agrícolas 11:1135-1147. https://doi.org/10.29312/remexca.v11i5.2325

Nirenberg HI. 1976. Untersuchungen über die morphologische und biologische differenzierung in der *Fusarium*-Sektion *Liseola*. Mitteilungen aus der Biologischen Bundesanstalt für Land- und Forstwirtschaft, Berlin-Dahlem. Kommissionsverlag Paul Parey, Berlin 169:1-117. https://doi.org/10.5073/20210624-085725

Okereke VC and Wokocha RC. 2007. *In vitro* growth of four isolates of *Sclerotium rolfsii* Sacc in the humid tropics. African Journal of Biotechnology 6:1879-1881. https://doi.org/10.5897/AJB2007.000-2279

Paparu P, Acur A, Kato F, Acam C, Nakibuule J, *et al*. 2020. Morphological and pathogenic characterization of *Sclerotium rolfsii*, the Causal agent of southern blight disease on common bean in Uganda. Plant Disease 104:2130-2137. https://doi.org/10.1094/PDIS-10-19-2144-RE

Paul SK, Mahmud NU and Gupta DR. 2021. Characterization of *Sclerotium rolfsii* Causing Root Rot of Sugar Beet in Bangladesh. Sugar Tech 23:1199–1205. https://doi.org/10.1007/s12355-021-00984-6

Prasad LS, Sujatha K, Naresh N and Chander SR. 2012. Variability in *Sclerotium rolfsii* associated with collar rot of sunflower. Indian Phytopathology 65:161-165. https://doi.org/10.13140/2.1.3722.8168

Punja ZK, Smith VL, Campbell CL and Jenkins SF. 1985. Sampling and extraction procedures to estimate numbers, spatial pattern, and temporal distribution of sclerotia of *Sclerotium rolfsii* in soil. Plant Disease 69:469-474.

Rai S, Kumar SM, Chandrol SA and Surapathrudu K. 2019. Biocontrol potential of *Trichoderma* spp.: current understandings and future outlooks on molecular techniques. In: Ansari, R., Mahmood, I. (eds) Plant Health Under Biotic Stress. Springer, Singapore. Plant Health Under Biotic Stress 7:129-160. https://doi.org/10.1007/978-981-13-6040-4_7

Rambaut A. 2014. FigTree v. 1.4: tree figure drawing tool. http://tree.bio.ed.ac.uk/software/figtree/

Rambaut A, Drummond AJ, Xie D, Baele G and Suchard MA. 2018. Posterior summarisation in Bayesian phylogenetics using Tracer 1.7. Systematic Biology 67: 901–904. https://doi.org/10.1093/sysbio/syy032

Roca LF, Raya MC, Luque F, Brisach CA, Romero J, *et al*. 2016. First Report of *Sclerotium rolfsii* causing soft rot of potato tubers in Spain. The American Phytopathological Society 100:2535-2535. https://doi.org/10.1094/PDIS-12-15-1505-PDN

Ronquist F, Teslenko M, Mark PVD, Ayres DL, Darling A, *et al*. 2012. MrBayes 3.2: efficient Bayesian phylogenetic inference and model choice across a large model space. Systematic Biology 61:539–542. https://doi.org/10.1093/sysbio/sys029

Rubayet MT and Bhuiyan MKA. 2016. Integrated management of stem rot of potato caused by *Sclerotium rolfsii.* Bangladesh Journal Plant Pathology 32:7-14.

https://www.researchgate.net/publication/328476753_INTEGRATED_MANAGEMENT_OF_STEM_ROT_OF_POTATO_CAUSED_BY_SCLEROTIUM_ROLFSII

Sanger F, Nicklen S and Coulson AR. 1977. DNA sequencing with chain-terminating inhibitors. Proceedings of the national academy of sciences of the United States of America 74:5463-5467. https://doi.org/10.1073/pnas.74.12.5463

Servicio de Información Agroalimentaria y Pesquera (SIAP). 2023. https://nube.siap.gob.mx/cierreagricola/ Consulta, enero 2024

Stamatakis A. 2006. RAxML-VI-HPC: maximum likelihood-based phylogenetic analyses with thousands of taxa and mixed models. Bioinformatics 22:2688-2690. https://doi.org/10.1093/bioinformatics/btl446

Van-Bezooijen J. 2006. Methods and techniques for nematology, revised version. Wageningen, Netherlands 54-55. http://www.nematologia.com.br/files/tematicos/5.pdf

White TJ, Bruns T, Lee S and Taylor J. 1990. Amplification and direct sequencing of fungal ribosomal rna genes for phylogenetics. Part Three. Genetics and Evolution. PCR Protocols 315-322. https://www.researchgate.net/publication/262687766_Amplification_and_Direct_Sequencing_of_Fungal_Ribosomal_RNA_Genes_for_Phylogenetics

Zhou L, Huang P, Yu L, Sun M and Fang Y. 2019. Southern blight on macleaya microcarpa caused by *Sclerotium rolfsii* in China. The American Phytopathological Society 103:2136-2136. https://doi.org/10.1094/PDIS-12-18-2172-PDN

Zúñiga M and Ceja-Torres LF. 2017. *In vitro* antagonism of *Trichoderma harzianum* on *Sclerotium cepivorum* Berk. and *S. rolfsii* Sacc., causal agents of onion rot. Phyton International Journal of Experimental Botany 86:7-13. https://doi.org/10.32604/phyton.2017.86.007